Title

Diffuse Midline Gliomas with Histone H3-K27M Mutation: A Series of 47 Cases Assessing the Spectrum of Morphologic Variation and Associated Genetic Alterations

Journal

Brain Pathology, 26(5)

ISSN

1015-6305

Authors

Solomon, David A
Wood, Matthew D
Tihan, Tarik
et al.

Publication Date

2016-09-01

DOI

10.1111/bpa.12336

Peer reviewed

Brain Pathology ISSN 1015–6305

RESEARCH ARTICLE

Diffuse Midline Gliomas with Histone H3-K27M Mutation: A Series of 47 Cases Assessing the Spectrum of Morphologic Variation and Associated Genetic Alterations

David A. Solomon[1]; Matthew D. Wood[1]; Tarik Tihan[1]; Andrew W. Bollen[1]; Nalin Gupta[2,3]; Joanna J. J. Phillips[1,2]; Arie Perry[1,2]

[1] Division of Neuropathology, Department of Pathology, University of California, San Francisco, CA.
[2] Department of Neurological Surgery, University of California.
[3] Department of Pediatrics, University of California.

Keywords
astrocytoma, diffuse midline glioma, diffuse intrinsic pontine glioma, DIPG, glioblastoma, histone H3.1, histone H3.3, H3F3A, HIST1H3B, K27M mutation.

Corresponding author:
Dr. Arie Perry, MD, Division of Neuropathology, University of California, San Francisco, 505 Parnassus Ave, Room M-551, San Francisco, CA 94143 (E-mail: *arie.perry@ucsf.edu)*

Received 22 September 2015
Accepted 26 October 2015
Published Online Article Accepted 30 October 2015

doi:10.1111/bpa.12336

Abstract

Somatic mutations of the *H3F3A* and *HIST1H3B* genes encoding the histone H3 variants, H3.3 and H3.1, were recently identified in high-grade gliomas arising in the thalamus, pons and spinal cord of children and young adults. However, the complete range of patients and locations in which these tumors arise, as well as the morphologic spectrum and associated genetic alterations remain undefined. Here, we describe a series of 47 diffuse midline gliomas with histone H3-K27M mutation. The 25 male and 22 female patients ranged in age from 2 to 65 years (median = 14). Tumors were centered not only in the pons, thalamus, and spinal cord, but also in the third ventricle, hypothalamus, pineal region and cerebellum. Patients with pontine tumors were younger (median = 7 years) than those with thalamic (median = 24 years) or spinal (median = 25 years) tumors. A wide morphologic spectrum was encountered including gliomas with giant cells, epithelioid and rhabdoid cells, primitive neuroectodermal tumor (PNET)-like foci, neuropil-like islands, pilomyxoid features, ependymal-like areas, sarcomatous transformation, ganglionic differentiation and pleomorphic xanthoastrocytoma (PXA)-like areas. In this series, histone H3-K27M mutation was mutually exclusive with *IDH1* mutation and *EGFR* amplification, rarely co-occurred with *BRAF-V600E* mutation, and was commonly associated with p53 overexpression, ATRX loss (except in pontine gliomas), and monosomy 10.

INTRODUCTION

Recent genomic analysis has demonstrated that specific genetic alterations drive distinct subsets of glial neoplasms of the central nervous system, dependent not only on tumor-type but also site of origin and patient age. For example, two independent studies in 2012 reported the identification of somatic mutation of the *H3F3A* and *HIST1H3B* genes, which encode the histone H3 variants H3.3 and H3.1, in pediatric diffuse intrinsic pontine gliomas (DIPG) and nonbrainstem glioblastomas (25, 29). A recurrent lysine to methionine substitution at codon 27 (K27M) was present in one of these two histone H3 variants in the majority of DIPGs and thalamic glioblastomas, whereas a recurrent glycine to arginine or valine substitution at codon 34 (G34R/V) was present in a subset of those pediatric nonmidline glioblastomas arising the cerebral hemispheres. Subsequent analyses have now demonstrated that histone H3-K27M mutations are present in the majority of high grade infiltrative astrocytomas arising within midline structures (thalamus, pons and spinal cord) of both pediatric and young adult patients (1, 5, 9, 11, 12, 19, 20, 24, 26). Studies have shown that these diffuse midline gliomas with histone H3-K27M mutation are associated with aggressive clinical behavior and poor prognosis (19, 20, 26), including those tumors which demonstrate only low grade histologic features on biopsy (5). However, more recent studies have shown that thalamic gliomas in adult patients with histone H3-K27M mutation might not be associated with worse prognosis than corresponding histone H3 wild-type thalamic gliomas (1, 9), suggesting heterogeneity among this molecular subgroup of diffuse midline gliomas.

Investigation has shown that this K27M mutation alters an important site of post-translational modification in the histone H3 variants and leads to altered DNA methylation and gene expression profiles thought to drive gliomagenesis (3, 7, 15, 21, 26). Thus, there are ongoing efforts to study the efficacy of therapeutics targeting histone modifying enzymes for these midline gliomas with histone H3 mutations. A recent preclinical study demonstrated remarkable efficacy with a novel small molecule inhibitor of the histone demethylase JMJD3 both *in vitro* and *in vivo* orthotopic xenograft models (14). A second group recently demonstrated

therapeutic efficacy with the histone deacetylase inhibitor panobinostat both *in vitro* and *in vivo* orthotopic xenograft models (13). It is, thus, important to identify those gliomas with histone H3 mutations, given the prognostic significance and potential targeted therapy that will soon be in clinical trials for these patients.

Genomic analysis of diffuse midline gliomas with histone H3-K27M mutations (K27M+) has revealed a number of cooperating genetic alterations. In particular, these tumors often also have *TP53* and *ATRX* mutations but do not have *IDH1* mutation (19, 25, 26). More recently, a subset of K27M+ DIPGs were found to also harbor missense mutations in the *ACVR1* gene, encoding the activin A receptor type-1 transmembrane protein, that lead to activation of the BMP-TGFβ signaling pathway (6, 10, 27, 30). Other alterations occasionally found in K27M+ DIPGs include *PIK3CA* mutation, *PDGFRA* mutation or amplification, *PPM1D* mutation, and amplification of cell cycle genes including *CCND1*, *CDK4* and *CDK6* (30, 31). The cooperating genetic alterations in nonbrainstem gliomas with histone H3-K27M mutation are less well defined, particularly in spinal cord and thalamic gliomas in adult patients. Notably, rare examples of midline glial neoplasms have been identified in pediatric patients that harbor both histone H3-K27M mutation and *BRAF-V600E* mutation (23). Accurate pathologic diagnosis in these cases was reportedly difficult, and two patients had long term survival of three or more years after diagnosis.

Additionally, the morphologic spectrum of K27M+ diffuse midline gliomas has only been reported in a limited fashion. In one assessment of six pediatric epithelioid glioblastomas, one tumor centered in the thalamus harbored a K27M mutation in *H3F3A*, suggesting that epithelioid features can occasionally be seen (4). Additionally, a recent case report described a tumor with histologic features resembling pilocytic astrocytoma arising in the cervical spinal cord of a seven-year-old girl that harbored histone H3-K27M mutation but lacked the characteristic *BRAF-KIAA1549* gene fusion (16). This patient had disease-free survival for 10 years following resection without additional therapy but subsequently had disease recurrence with malignant transformation causing her eventual death 12 months later. Such cases suggest that this molecular subgroup of diffuse midline gliomas is not morphologically uniform.

In this study, we report clinicopathologic assessment of 73 infiltrative gliomas and 15 pilocytic astrocytomas centered in midline structures in both pediatric and adult patients, including immunohistochemistry with a recently developed mutant-specific antibody that accurately detects the K27M mutation of both histone H3.3 and histone H3.1 (2, 28). Our findings highlight the range of midline locations and patients in which gliomas with histone H3-K27M mutation arise, as well as demonstrate the diverse histopathologic spectrum that can be observed in this molecular subgroup of diffuse midline gliomas.

MATERIAL AND METHODS

Tumor samples and histologic review

This study was performed in accordance with guidelines set forth by the institutional review board of the University of California, San Francisco (UCSF). For all tumors, formalin-fixed paraffin-embedded tumor tissue was prospectively examined from both UCSF in-house and consults cases over a one-year period. Hematoxylin and eosin (H&E) stained sections were reviewed for diagnostic assessment and determination of morphologic variation. Among the 47 K27M+ diffuse midline gliomas, 17 of the pediatric cases and 10 of the adult cases were resected in-house, whereas 10 of the pediatric cases and 10 of the adult cases were resected at outside institutions and reviewed at UCSF in consultation.

Immunohistochemistry and fluorescence *in situ* hybridization (FISH)

Immunohistochemistry was performed on formalin-fixed, paraffin embedded tissue sections at the UCSF Immunohistochemistry Laboratory and the UCSF Neuropathology BTRC Biomarkers Laboratory. Primary antibodies used were as follows: histone H3-K27M mutant protein (ABE419, EMD Millipore, Billerica, MA, 1:500 dilution), IDH1-R132H mutant protein (clone H09, DiaNova, Germany, 1:500 dilution), ATRX (HPA001906, Sigma, St Louis, MO, 1:100 dilution), p53 (clone DO-7, Dako, Glostrup, Denmark, 1:00 dilution), BRAF-V600E mutant protein (clone VE1, Ventana, Tucson, AZ). All staining was performed in Ventana or Leica Bond automated staining processors. Specifically, the histone H3-K27M immunostaining was run in a Ventana Benchmark XT autostainer using CC1 antigen retrieval buffer for 30 minutes at 95°C, incubation with 1:500 dilution of primary antibody for 32 minutes, and Ventana ultraView Universal DAB detection. Dual-color FISH for EGFR and CEP7 or PTEN and CEP10 was performed on 5-micron thick FFPE whole sections as previously described (17).

RESULTS

Immunohistochemistry for histone H3-K27M mutant protein was performed on a total of 73 infiltrative gliomas arising in midline locations, 21 infiltrative gliomas arising in the cerebral hemispheres and 15 pilocytic astrocytomas arising in midline locations (Table 1).

Table 1. IHC results for histone H3-K27M mutant protein.

	K27M+	K27M–	Total	% K27M+
Infiltrative gliomas				
Pons	17	1	18	94%
Thalamus	15	8	23	65%
Spinal cord	9	8	17	53%
Third ventricle	3	0	3	100%
Hypothalamus	1	3	4	25%
Cerebellum	1	3	4	25%
Pineal region	1	1	2	50%
Cerebral hemispheres	0	21	21	0%
Midbrain	0	1	1	0%
Medulla	0	1	1	0%
Total for midline sites	47	26	73	64%
Total for all sites	47	47	94	50%
Pilocytic astrocytomas				
Spinal cord	0	5	5	0%
Cerebellum	0	4	4	0%
Tectum	0	3	3	0%
Third ventricle	0	1	1	0%
Hypothalamus	0	1	1	0%
Medulla	0	1	1	0%
Total for all sites	0	15	15	0%

Table 2. Clinical and molecular features of diffuse midline gliomas with histone H3-K27M mutation.

			Patient age (yrs)		Surgery		WHO grade			Immunohistochemistry				FISH	
Tumor site	Cases	Sex (M: F)	Median	Range	Biopsy	Resection	II	III	IV	IDH1-R132H+	ATRX loss	p53+	BRAF-V600E+	EGFR amp	ch 10 loss
Pons	17	8:9	7	4–24	16	1	5	8	4	0/10	1/13	4/12	0/7	0/4	2/4
Thalamus	15	7:8	24	2–60	11	4	1	4	10	0/11	9/12	8/13	1/4	0/6	1/6
Spinal cord	9	5:4	25	4–41	4	5	3	0	6	0/6	4/7	1/5	0/4	0/2	1/2
Third ventricle	3	2:1	19	14–33	1	2	1	1	1	0/2	1/2	0/1	0/2	0/1	0/1
Hypothalamus	1	1:0	30	–	1	0	0	0	1	0/1	0/1	1/1	–	0/1	0/1
Cerebellum	1	1:0	9	–	0	1	0	0	1	–	–	–	–	–	–
Pineal region	1	1:0	65	–	1	0	0	1	0	–	0/1	0/1	0/1	0/1	0/1
Total	47	25:22	14	2–65	34	13	10	14	23	0/30	15/32	14/33	1/18	0/15	4/15

WHO grade refers to histology at time of initial biopsy or resection.
p53+ refers to strong nuclear p53 staining in the majority of tumor cells.
EGFR amp refers to high level amplification of EGFR with >10 copies per cell.

Forty-seven of the 73 infiltrative gliomas (64%) arising in midline locations were positive for histone H3-K27M mutant protein, while none of the 21 infiltrative gliomas arising in the cerebral hemispheres or 15 pilocytic astrocytomas were positive.

Among the midline infiltrative gliomas, histone H3-K27M mutant protein was detected in 17 of 18 (94%) pontine, 15 of 23 (65%) thalamic, nine of 17 (53%) spinal, three of three (100%) third ventricular, one of four (25%) hypothalamic, one of four (25%) cerebellar, one of two (50%) pineal, zero of one (0%) midbrain (0%), and zero of one (0%) medulla-centered gliomas.

Clinical features of diffuse midline gliomas with histone H3-K27M mutation

Among the 47 patients with diffuse midline gliomas positive for histone H3-K27M mutation, 25 were males and 22 were females (Table 2). Patient age at time of diagnosis ranged from 2 to 65 years old with a median age of 14 years. Patients with pontine gliomas were younger (median = 7 years) than those with thalamic (median = 24 years) or spinal (median = 25 years) gliomas (Figure 1).

Thirty-four of these 47 patients underwent biopsy only, whereas 13 underwent resection (Table 2). Initial histologic diagnosis was diffuse astrocytoma (WHO grade II) in 10 cases, anaplastic astrocytoma (WHO grade III) in 14 cases and glioblastoma (WHO grade IV) in 23 cases. During the short period of clinical follow-up, five of these patients underwent a subsequent biopsy or resection demonstrating higher grade gliomas. These included two pontine gliomas originally classified as grade III that were upgraded to glioblastoma, a spinal glioma and a third ventricle glioma originally classified as grade II that were upgraded to glioblastoma, and a thalamic glioma originally classified as grade II that was upgraded to anaplastic astrocytoma.

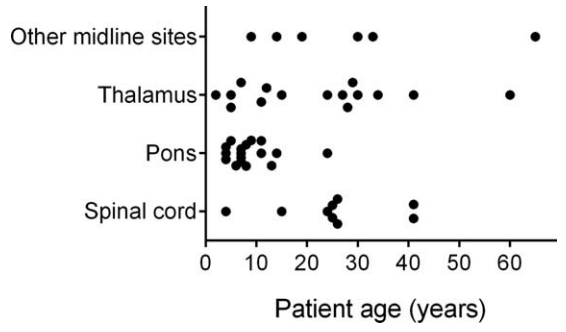

Figure 1. Age distribution of the 47 patients with diffuse midline gliomas with histone H3-K27M mutation at time of initial diagnosis plotted by tumor site. Pons, 17 cases; thalamus, 15 cases; spinal cord, nine cases; other midline sites, six cases.

Given the prospective nature of this study without significant length of clinical follow-up, the utility of assessing outcome measures including recurrence-free survival and overall survival in this patient cohort is limited at present. A follow-up study will assess these clinical parameters to evaluate for differences in clinical outcome based on histone H3-K27M mutation status, tumor site, patient age, associated molecular alterations and other variables in this patient cohort.

Histologic features of diffuse midline gliomas with histone H3-K27M mutation

In assessing the morphologic features of these 47 diffuse midline gliomas with histone H3-K27M mutation, all tumors had at least some classic astrocytic morphology with ovoid to elongate nuclei containing coarse chromatin. None had widespread oligodendroglial morphology with uniform round nuclei and more delicate chromatin warranting classification as oligodendroglioma. In each case, histone H3-K27M mutant protein staining was diffusely positive throughout all tumor nuclei, suggesting that histone H3 mutation is an early or initiating event in these diffuse midline gliomas. Additionally, histone H3-K27M positivity was limited to the neoplastic cells in all cases, with no nuclear staining seen in endothelial cells, inflammatory cells, or entrapped non-neoplastic neurons and glial cells. As a potential diagnostic pitfall, nonspecific cytoplasmic staining was often seen in admixed macrophages and microglial cells in tumors lacking histone H3-K27M mutant protein (Figure 2), although this pattern was easy to distinguish from the nuclear staining seen in positive tumor cells. A representative example of a diffuse midline glioma with histone H3-K27M mutation arising in the pons of an eight-year-old boy is shown in Figure 3. An autopsy

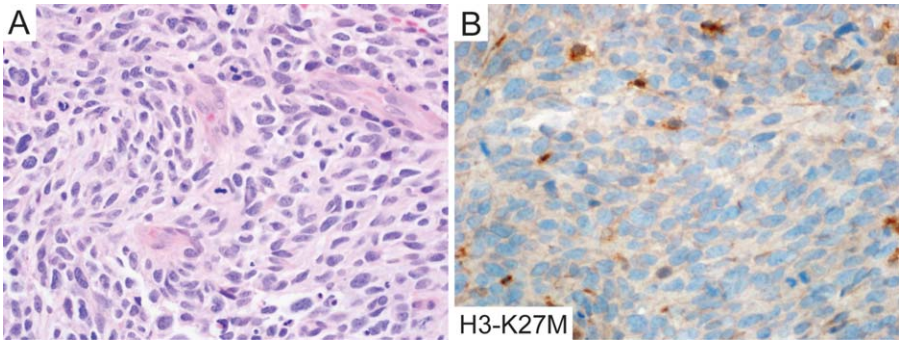

Figure 2. *Example of a diffuse midline glioma negative for histone H3-K27M mutation.* **A.** H&E stained section of a glioblastoma arising in the medulla of a 46-year-old man. **B.** Immunohistochemistry for histone H3-K27M mutant protein showed nonspecific cytoplasmic staining in admixed microglia and macrophages with no staining of tumor nuclei.

was performed on this patient following palliative radiation and chemotherapy, and histone H3-K27M immunohistochemistry was helpful in assessing the widespread infiltration of the tumor cells throughout the brain and spinal cord. Tumor cells were seen infiltrating from the brainstem into multiple cranial nerves (Figures 3H and I), a finding that has only been rarely observed in malignant gliomas (22).

While the vast majority of diffuse midline gliomas with histone H3-K27M mutation previously reported have been centered in the thalamus, pons or spinal cord, we identified six malignant gliomas arising in other midline sites including the third ventricle, hypothalamus, pineal region and cerebellum (Figure 4). All of these tumors displayed typical morphologic features of infiltrative astrocytomas, except for one glioblastoma arising in the third ventricle of a 19-year-old woman with tumor cells that contained clear cytoplasm and distinct cell borders (Figures 4G–I).

Among the 41 diffuse midline gliomas with histone H3-K27M mutation arising in the thalamus, pons and spinal cord, a wide spectrum of morphologic variation was encountered (Figures 5–7). Two glioblastomas had frequent giant cells, including one arising in the pons of a 7-year-old girl and one arising in the thalamus of a 12-year-old girl (Figures 5A and B), both of which showed p53 overexpression in the majority of tumor nuclei. One glioblastoma arising in the cervical spinal cord of a 15-year-old boy demonstrated prominent pilomyxoid features with rather monomorphic piloid astrocytes radially arranged vessels in a prominent myxoid stroma, resembling pilomyxoid astrocytoma. Other areas of the tumor demonstrated increased cellularity and pleomorphism with brisk mitotic activity and microvascular proliferation, which together with the histone H3-K27M positivity, warranted classification as glioblastoma, WHO grade IV (Figures 5C and D). Another notable glioblastoma arising in the thalamus of a 27-year-old woman demonstrated epithelioid features and also contained primitive neuroectodermal tumor (PNET)-like foci (Figures 5E–H).

Another interesting glioma variant we observed to harbor histone H3-K27M mutation was a glioblastoma with neuropil-like islands arising in the thoracic spinal cord of a 25-year-old woman (Figures 6A–C). This tumor contained neuropil-like islands as highlighted by synaptophysin immunohistochemistry circumferentially surrounded by neoplastic astrocytes. Other areas of the tumor contained necrosis and microvascular proliferation, warranting classification as glioblastoma. As opposed to the vast majority of the diffuse gliomas with neuropil-like islands that have been reported to date (18), this tumor lacked IDH1 mutant protein. One gliosarcoma arising in the thalamus of an 11-year-old girl highlighted the spectrum of intratumoral variation that can be observed in diffuse midline gliomas with histone H3-K27M mutation. Portions of this tumor were composed of ependymal-like areas with solid growth, uniform ovoid nuclei, no mitotic activity, abundant dystrophic calcification, perivascular pseudorosettes and cytoplasmic dot-like immunohistochemical staining for epithelial membrane antigen (EMA; Figures 6D–F). These low grade areas were adjacent to more anaplastic appearing areas composed of spindled cells with fascicular growth, brisk mitotic activity and loss of markers of glial differentiation such as GFAP and OLIG2 suggestive of sarcomatous transformation (Figures 6G–I). Another morphologic variant was a malignant glioma with epithelioid to rhabdoid features and ganglionic differentiation in the thoracic spinal cord of a 26-year-old man. The majority of this tumor was composed of loosely cohesive cells with eccentric nuclei and abundant eosinophilic cytoplasm, many of which contained spherical intracytoplasmic inclusions (Figures 6J–L). One area of the tumor demonstrated numerous large atypical ganglion-like cells which were also positive for histone H3-K27M mutant protein (Figures 6M–O). The classification of this tumor remained enigmatic, though we favored that it represents a diffuse midline glioma with epithelioid/rhabdoid features and ganglionic differentiation rather than an anaplastic ganglioglioma with malignant glial component demonstrating features of epithelioid/rhabdoid glioblastoma.

Molecular features of diffuse midline gliomas with histone H3-K27M mutation

As part of the clinical workup of these 47 diffuse midline gliomas with histone H3-K27M mutation, a combination of additional molecular testing was variably performed including immunohistochemistry for ATRX, p53, IDH1-R132H mutant protein and BRAF-V600E mutant protein, as well as FISH for EGFR and PTEN genes (Table 2). ATRX immunostaining revealed loss of nuclear expression in 15 of 32 tested cases, including nine of 12 thalamic gliomas (75%), four of seven spinal gliomas (57%), and one of 13 pontine gliomas (8%). Of the 33 cases assessed, 14 demonstrated strong p53 immunoreactivity in the majority of tumor nuclei suggestive of TP53 gene mutation or other mechanism of p53 stabilization. Whereas ATRX loss was more commonly seen in the thalamic and spinal gliomas, p53 overexpression was more frequent in the thalamic (eight of 13 cases, 62%) vs. pontine (four of 12 cases, 33%) and spinal gliomas (one of five cases, 20%). No significant correlation between tumor grade and ATRX or p53 status was seen in this cohort. Of the 30 cases tested for IDH1-R132H mutant protein, none were positive. Only one of the 18 cases tested

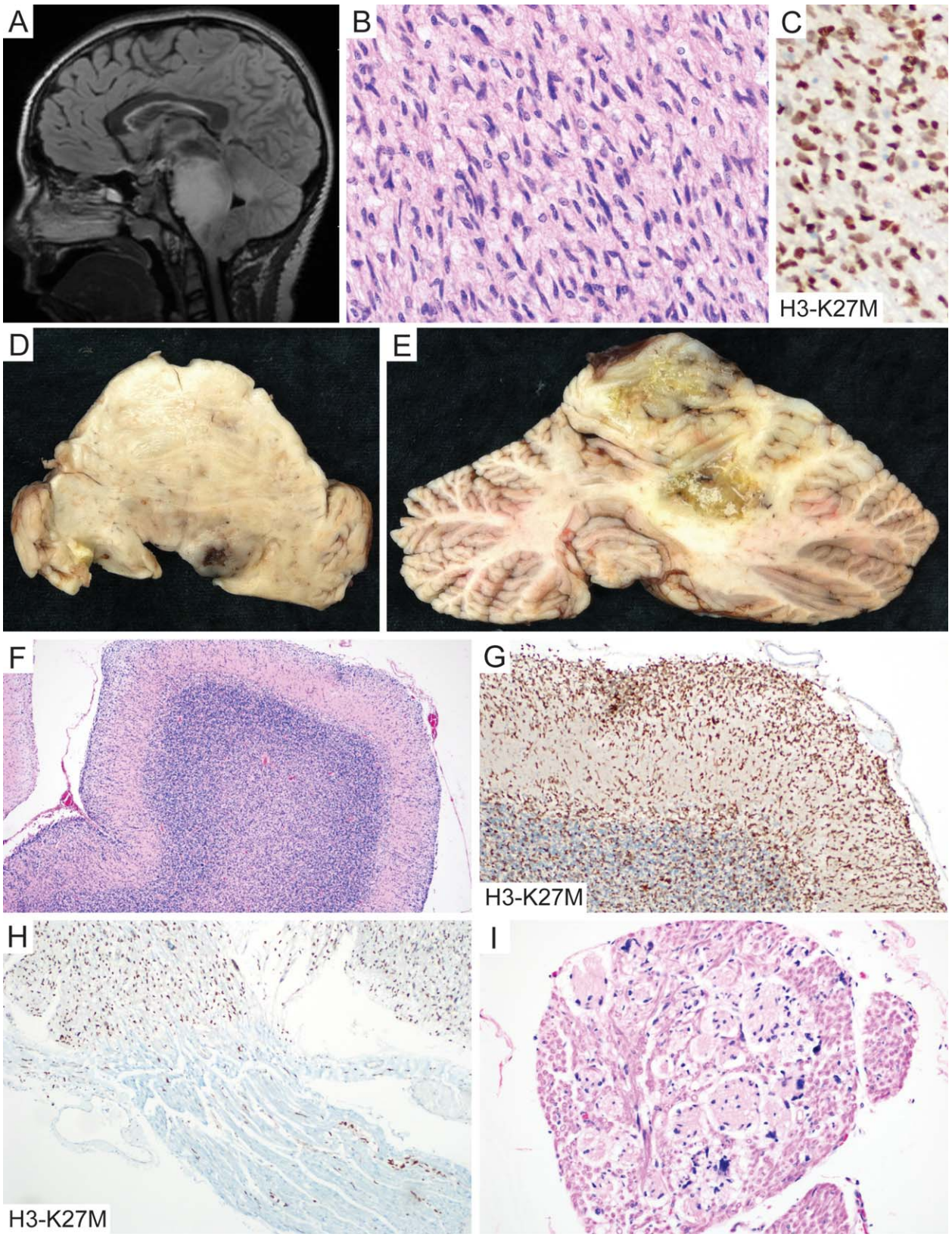

Figure 3. *Pathologic features of a diffuse midline glioma with histone H3-K27M mutation arising in the pons in an 8-year-old boy from the initial biopsy and at autopsy following palliative radiation and chemotherapy*. **A.** Mid-sagittal T2 FLAIR image at time of presentation demonstrating a nonenhancing, T2-hyperintense mass expanding the pons with probable infiltration into the adjacent cerebellum. **B.** H&E stained section from a diagnostic biopsy performed at the time of presentation showing a highly cellular infiltrative astrocytoma with scattered mitotic figures. **C.** Immunohistochemical stain for histone H3-K27M mutant protein showing strong nuclear positivity in tumor cells. **D,E.** Gross photographs of an axial section through the pons (D) and coronal section through the cerebellum (E) from the autopsy performed 12 months after the initial diagnostic biopsy following palliative radiation and chemotherapy with bevacizumab. The pons and cerebellum are markedly expanded and distorted by the tumor and show multiple foci of radiation-induced necrosis. **F,G.** H&E stained section from the left cerebellar cortex and corresponding immunohistochemical stain for histone H3-K27M mutant protein showing massive infiltration by neoplastic astrocytes with prominent subpial accumulation. **H.** Immunohistochemical stain for histone H3-K27M from the midbrain highlights cranial nerve infiltration by the tumor cells. **I.** H&E stained cross-section of a cranial nerve showing numerous neoplastic astrocytes within the endoneurium.

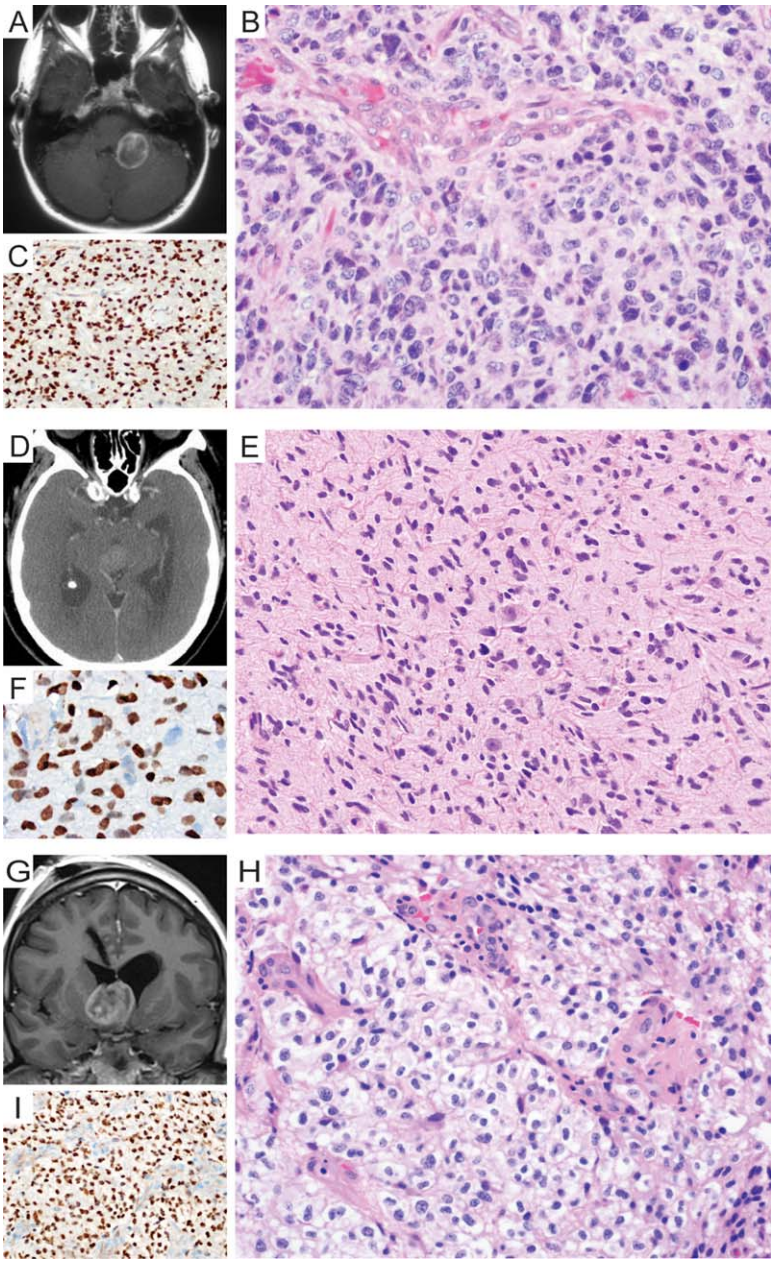

Figure 4. *Examples of diffuse midline gliomas with histone H3-K27M mutation arising in midline sites other than the thalamus, pons, or spinal cord.* **A–C.** Glioblastoma arising in the cerebellum of a 9-year-old boy. (A) Preoperative axial T1 postcontrast MR image demonstrating a peripherally enhancing mass within the left cerebellar white matter and cerebellar peduncle. H&E stained section showing a highly pleomorphic infiltrating astrocytoma with microvascular proliferation (B), and immunohistochemical stain for histone H3-K27M mutant protein showing strong nuclear positivity in tumor cells (C). **D–F.** Anaplastic astrocytoma centered in the pineal region of a 65-year-old man. (D) Preoperative axial postcontrast CT image demonstrating a faintly enhancing mass in the pineal region. H&E stained section showing an infiltrative astrocytoma with scattered mitotic figures (E), and immunohistochemical stain for histone H3-K27M mutant protein showing strong nuclear positivity in tumor cells (F). **G–I.** Glioblastoma arising in the third ventricle in a 19-year-old woman. (G) Coronal T1 postcontrast MR image taken following stereotactic biopsy showing a peripherally enhancing mass centered in the third ventricle near the foramen of Monro. H&E stained section showing an infiltrative astrocytoma with clear cytoplasm and well-developed microvascular proliferation (H), and immunohistochemical stain for histone H3-K27M mutant protein showing strong nuclear positivity in tumor cells.

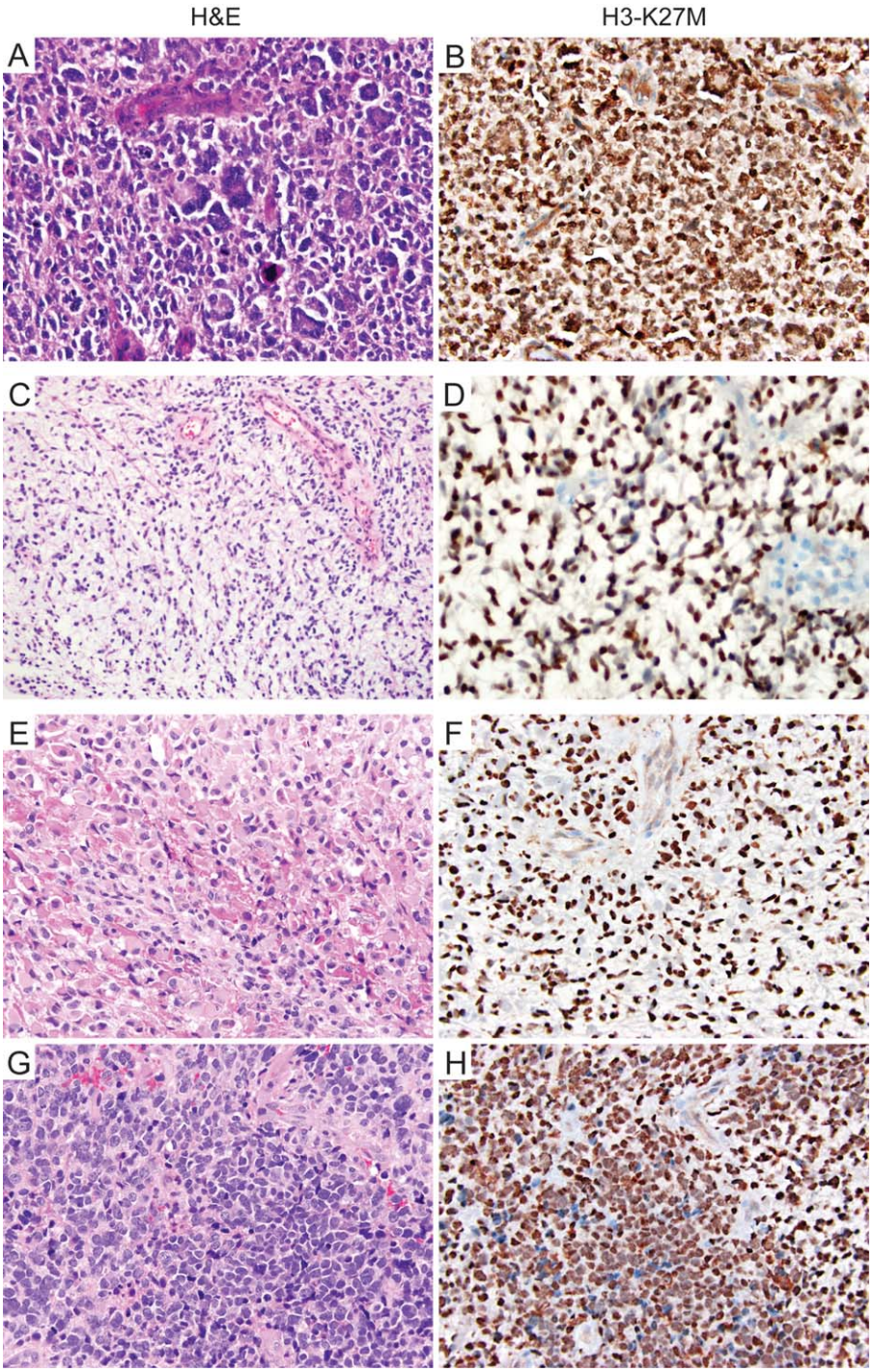

Figure 5. *Examples of morphologic variation encountered in diffuse midline gliomas with histone H3-K27M mutation.* **A,B.** Glioblastoma with frequent giant cells arising in the thalamus of a 12-year-old girl. **C,D** Glioblastoma with pilomyxoid features arising in the cervical spinal cord of a 15-year-old boy which demonstrates monomorphic piloid astrocytes radially arranged vessels in a prominent myxoid stroma. Other areas of the tumor demonstrated increased cellularity and pleomorphism with brisk mitotic activity and microvascular proliferation (not shown). **E–H.** Epithelioid glioblastoma with PNET-like foci arising in the thalamus of a 27-year-old woman. The majority of the tumor was composed of epithelioid astrocytes with abundant eosinophilic cytoplasm and distinct cell borders (E), with a smaller component of PNET-like foci composed of more primitive appearing cells with scant cytoplasm, nuclear molding, and brisk mitotic activity (G). H&E stained sections are shown in A, C, E and G, and corresponding immunohistochemical stained sections for histone H3-K27M mutant protein are shown in B, D, F and H.

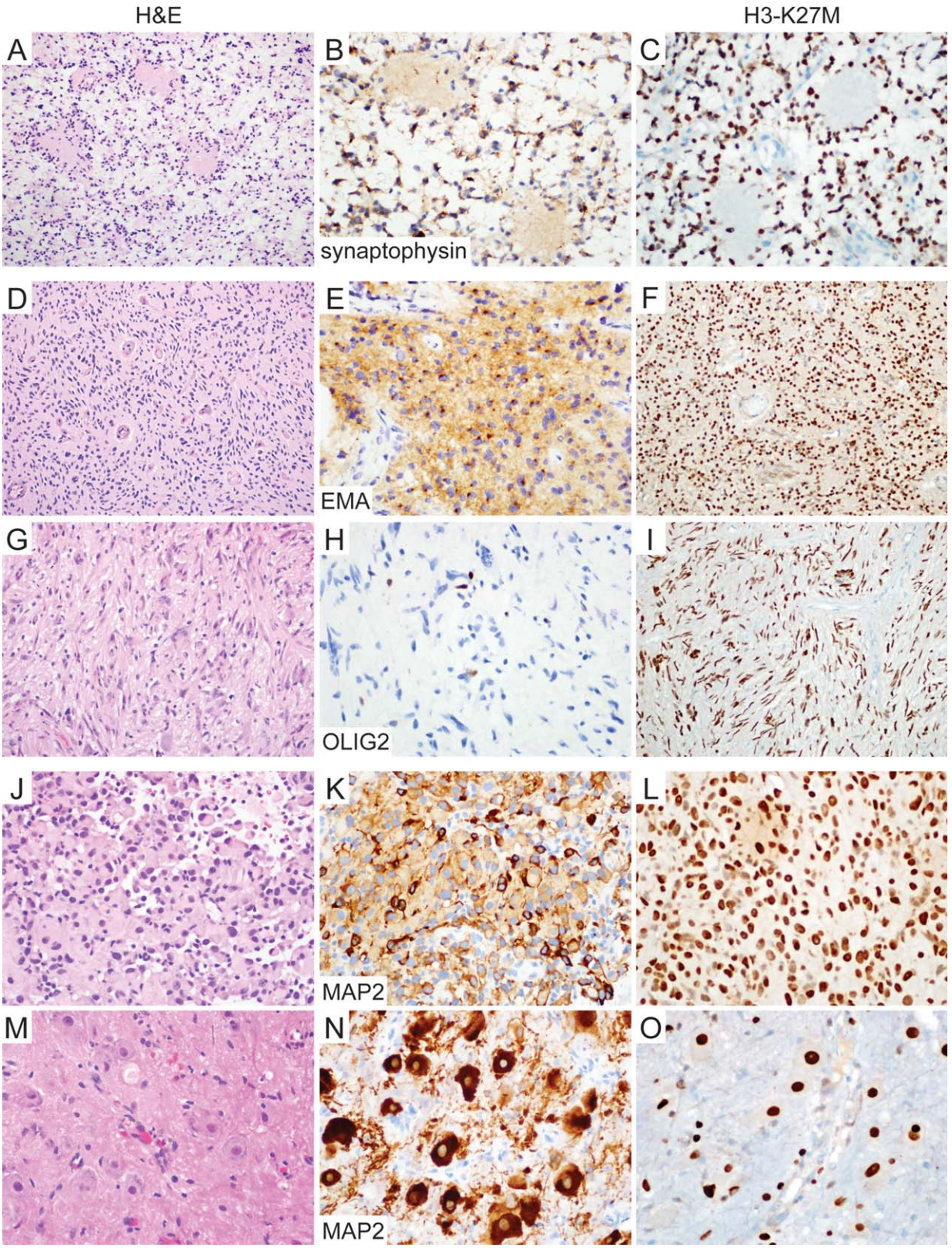

Figure 6. *Additional examples of morphologic variation encountered in diffuse midline gliomas with histone H3-K27M mutation.* **A–C.** Glioblastoma with neuropil-like islands arising in the thoracic spinal cord of a 25-year-old woman. The tumor contained frequent neuropil-like islands, highlighted by synaptophysin immunohistochemistry (B), circumferentially surrounded by neoplastic astrocytes. Other areas of the tumor contained necrosis and microvascular proliferation (not shown). **D–I.** Gliosarcoma with ependymal-like areas arising in the thalamus of an 11-year-old girl. Areas within the tumor showed solid growth with uniform ovoid nuclei, no mitotic activity, and perivascular arrangement resembling the pseudorosettes seen in ependymomas (D). Immunohistochemical staining for EMA in these areas of the tumor demonstrated dot-like cytoplasmic positivity (E). Other areas showed a more anaplastic sarcoma-like component with fascicles of spindled cells and brisk mitotic activity (G) that demonstrated increased intercellular reticulin deposition (not shown) and loss of markers of glial differentiation, including OLIG2 (H). Strong nuclear staining for histone H3-K27M mutant protein was seen diffusely throughout the tumor including both the ependymal-like (F) and sarcomatous components (I). **J–O.** Malignant glioma with epithelioid/rhabdoid features and ganglionic differentiation arising in the thoracic spinal cord of a 26-year-old man. The majority of the tumor was composed of loosely cohesive cells with eccentric nuclei and abundant eosinophilic cytoplasm, many of which contain spherical intracytoplasmic inclusions (J). Immunohistochemistry for MAP2 showed cytoplasmic staining in the majority of cells with absence of staining in these paranuclear inclusions (K). One area of the tumor demonstrated numerous large atypical ganglion-like cells (M), which demonstrated strong cytoplasmic positivity on MAP2 immunostaining (N), as well as immunoreactivity for neurofilament and synaptophysin (not shown). Strong nuclear staining for histone H3-K27M mutant protein was seen diffusely throughout the tumor including both the epithelioid/rhabdoid cells (L) and the ganglion-like tumor cells (O).

for BRAF-V600E mutant protein was positive, which was the exceptional glioma arising in the thalamus of a 5-year-old girl depicted in Figure 7. This case demonstrated areas of both a diffusely infiltrative glioma admixed with other solid areas resembling pleomorphic xanthoastrocytoma (PXA), including nuclear pleomorphism out of proportion to mitotic activity, dense reticulin network, eosinophilic granular bodies, and CD34 positive stellate cells. Of 15 cases assessed by FISH, none had *EGFR* amplification while four had loss of chromosome 10, including a pontine glioblastoma in an 11-year-old boy, a pontine glioblastoma in a 4-year-old boy, a thalamic glioblastoma in a 24-year-old woman, and a glioma in the lumbar spinal cord with grade II histologic features at time of initial biopsy but grade IV histologic features on subsequent resection.

Characteristics of diffuse midline gliomas without histone H3-K27M mutation

Twenty-six of the 73 diffuse midline gliomas evaluated were negative for histone H3-K27M mutant protein expression. These included one of 18 tumors (6%) arising in the pons, 8 of 23 (35%) arising in the thalamus, eight of 17 (47%) arising in the spinal cord, three of four (75%) arising in the hypothalamus, three of four (75%) arising in the cerebellum, one of two (50%) arising in the pineal region, one of one (100%) arising in the midbrain, and one of one (100%) arising in the medulla. Two of these tumors (a glioblastoma in the thalamus of a 40-year-old woman and a glioblastoma in the hypothalamus of a 57-year-old man) had *EGFR* amplification and chromosome 10 deletions, similar to those more typically arising in the cerebral hemispheres. However, the molecular underpinnings of the rest of these tumors remains unknown, and none of the 19 tested cases had *IDH1* mutation.

Notably, three of these diffuse midline gliomas lacking histone H3-K27M mutation had a history of prior radiation therapy. These included the only K27M negative DIPG in this study that occurred in a 15-year-old boy after receiving craniospinal irradiation at 5 years of age following resection of a medulloblastoma from the midline of the posterior fossa. The second patient was a 35-year-old woman with glioblastoma centered in the thalamus who had received focused radiation to the pineal region four years prior following resection of a pineal parenchymal tumor. The third patient was a 46-year-old woman with a glioblastoma arising in the thoracic spinal cord following prior radiation therapy for Hodgkin's lymphoma.

DISCUSSION

"Diffuse midline glioma with histone H3-K27M mutation" is a distinct subtype of infiltrative glioma that will be recognized as a new diagnostic entity in the forthcoming 2016 edition of the *World Health Organization Classification of Tumors of the Central Nervous System* that utilizes integrated diagnosis incorporating both morphologic and molecular features. Emerging evidence indicates that these tumors arise in the thalamus, pons and spinal cord of children and young adults and are associated with poor prognosis. Given the prognostic implications and the new targeted therapies being developed for these gliomas with histone H3 gene mutations, there is increasing importance for recognition of this distinct glioma entity by diagnostic pathologists. We sought to determine the complete range of patients and locations in which these gliomas with histone H3-K27M mutation arise, as well as the morphologic spectrum and associated genetic alterations that can be seen in these tumors.

We identified 47 patients with diffuse midline gliomas harboring histone H3-K27M mutation. While all prior examples have been in pediatric and young adult patients, we found K27M+ gliomas in older adults up to 65 years of age. While nearly all prior examples of diffuse gliomas with histone H3-K27M mutation have been located in the thalamus, pons or spinal cord, we also found examples arising in the third ventricle, hypothalamus, pineal region and cerebellum. Furthermore, we note that a wide morphologic spectrum can be encountered, with features overlapping nearly every known histologic variant of infiltrative glioma and even some of the more circumscribed subtypes such as ganglioglioma and PXA.

In this series of 47 diffuse midline gliomas, histone H3-K27M mutation was mutually exclusive with *IDH1*-R132H mutation and *EGFR* amplification, rarely co-occurred with *BRAF-V600E* mutation, and was commonly associated with p53 overexpression, ATRX loss, and monosomy 10. Among these K27M+ diffuse

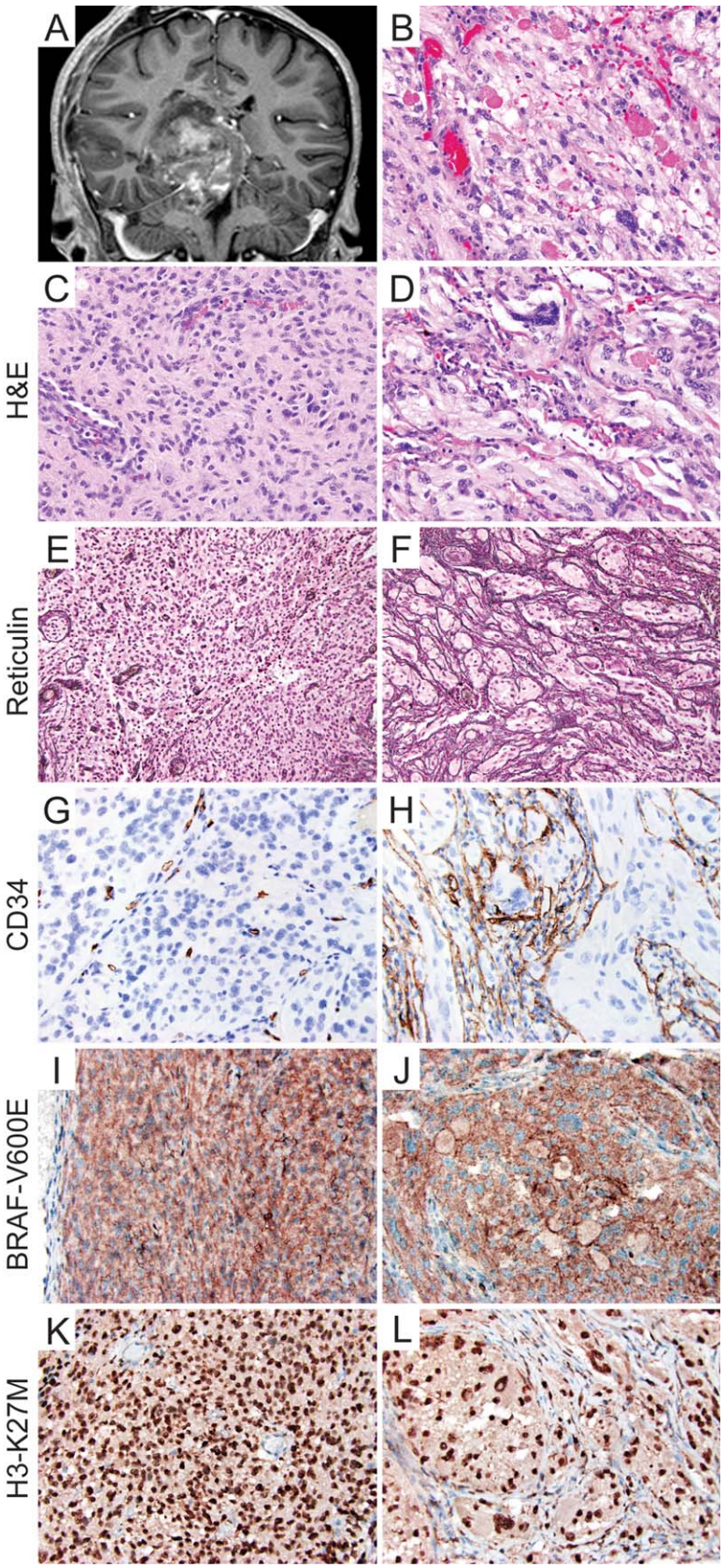

Figure 7. *Diffuse midline glioma with focal PXA-like features and both histone H3-K27M and BRAF-V600E mutation arising in the thalamus of a 5-year-old girl.* **A.** Preoperative coronal T1 postcontrast MR image demonstrating a complex, enhancing multinodular mass centered in the right thalamus with infiltration into the surrounding brain parenchyma. **B,D.** A large component of the tumor demonstrated histologic features of PXA with pleomorphic astrocytes, fascicular to storiform architecture, solid growth pattern, numerous eosinophilic granular bodies, and occasional xanthomatous cells. These PXA-like areas were in apposition to a diffusely infiltrative astrocytoma with scattered mitotic figures and infarct-like necrosis not associated with palisading or microvascular proliferation **C.** The diffusely infiltrative component of the tumor lacked significant reticulin deposition **(E)** and had CD34 immunostaining limited to endothelial cells **(G)**, while the PXA-like areas had a dense intercellular reticulin network **(F)** and interspersed stellate cells with CD34 staining **H.** Staining for both BRAF-V600E and histone H3-K27M mutant proteins was seen diffusely throughout the tumor including both the infiltrative component **(I,K)** and the PXA-like component **(J,L)**.

midline gliomas, ATRX loss was more common in thalamic and spinal tumors vs. pontine tumors, whereas p53 overexpression was most frequent in thalamic gliomas compared with the other sites. Whether these molecular differences between different anatomic locations reflects distinct glioma subgroups with divergent clinical outcomes remains to be determined, but this finding further substantiates the concept that K27M+ diffuse midline gliomas are a heterogeneous group of tumors, both morphologically and genetically.

We identified no diffuse gliomas arising in the cerebral hemispheres and no midline pilocytic astrocytomas with histone H3-K27M mutation. A subset of the diffuse midline gliomas we assessed was negative for histone H3-K27M mutant protein. While some of these tumors had molecular features similar to those seen in glioblastomas arising in the cerebral hemispheres (eg, *EGFR* amplification, *PTEN* deletion), the majority lacked known glioma molecular alterations including *EGFR* amplification, *IDH1* mutation and ATRX loss. These K27M negative diffuse midline gliomas included all of the three radiation-associated gliomas evaluated in this study, providing further support for the concept that radiation-induced gliomas are driven by a set of genetic alterations distinct from sporadic gliomas (8).

In summary, we recommend a liberal use of immunohistochemistry for clinical detection of histone H3-K27M mutation in all diffuse midline gliomas regardless of patient age. Given that diffuse midline gliomas with histone H3-K27M mutation can display a wide spectrum of morphologic variations, this immunostain may also be useful in midline glial and glioneuronal neoplasms with unusual morphologic patterns that would not previously have been considered part of the diffuse midline glioma family of tumors.

ACKNOWLEDGMENTS

We thank the UCSF Neuropathology BTRC Biomarkers Laboratory for developing and performing the immunohistochemical stain for histone H3-K27M mutant protein. D.A.S. is supported by a Career Development Award from the UCSF Brain Tumor SPORE and an NIH Director's Early Independence Award (DP5 OD021403).

REFERENCES

1. Aihara K, Mukasa A, Gotoh K, Saito K, Nagae G, Tsuji S *et al* (2014) H3F3A K27M mutations in thalamic gliomas from young adult patients. *Neuro Oncol* **16**:140–146.
2. Bechet D, Gielen GG, Korshunov A, Pfister SM, Rousso C, Faury D *et al* (2014) Specific detection of methionine 27 mutation in histone 3 variants (H3K27M) in fixed tissue from high-grade astrocytomas. *Acta Neuropathol* **128**:733–741.
3. Bender S, Tang Y, Lindroth AM, Hovestadt V, Jones DT, Kool M *et al* (2013) Reduced H3K27me3 and DNA hypomethylation are major drivers of gene expression in K27M mutant pediatric high-grade gliomas. *Cancer Cell* **24**:660–672.
4. Broniscer A, Tatevossian RG, Sabin ND, Klimo P Jr, Dalton J, Lee R *et al* (2014) Clinical, radiological, histological and molecular characteristics of paediatric epithelioid glioblastoma. *Neuropathol Appl Neurobiol* **40**:327–336.
5. Buczkowicz P, Bartels U, Bouffet E, Becher O, Hawkins C (2014) Histopathologic spectrum of paediatric diffuse intrinsic pontine glioma: diagnostic and therapeutic implications. *Acta Neuropathol* **128**: 573–581.
6. Buczkowicz P, Hoeman C, Rakopoulos P, Pajovic S, Letourneau L, Dzamba M *et al* (2014) Genomic analysis of diffuse intrinsic pontine gliomas identifies three molecular subgroups and recurrent activating ACVR1 mutations. *Nature Genet* **46**:451–456.
7. Chan KM, Fang D, Gan H, Hashizume R, Yu C, Schroeder M *et al* (2013) The histone H3.3-K27M mutation in pediatric glioma reprograms H3K27 methylation and gene expression. *Genes Dev* **27**:985–990.
8. Donson AM, Erwin NS, Kleinschmidt-DeMasters BK, Madden JR, Addo-Yobo SO, Foreman NK (2007) Unique molecular characteristics of radiation-induced glioblastoma. *J Neuropathol Exp Neurol* **66**: 740–749.
9. Feng J, Hao S, Pan C, Wang Y, Wu Z, Zhang J *et al* (2015) The H3.3 K27M mutation results in a poorer prognosis in brainstem gliomas than thalamic gliomas in adults. *Human Pathol.* [Epub ahead of print].
10. Fontebasso AM, Papillon-Cavanagh S, Schwartzentruber J, Nikbakht H, Gerges N, Fiset PO *et al* (2014) Recurrent somatic mutations in ACVR1 in pediatric midline high-grade astrocytoma. *Nature Genet* **46**: 462–466.
11. Gessi M, Gielen GH, Dreschmann V, Waha A, Pietsch (2015) High frequency of H3F3A (K27M) mutations characterizes pediatric and adult high-grade gliomas of the spinal cord. *Acta Neuropath* **130**: 435–437.
12. Gielen GH, Gessi M, Hammes J, Kramm CM, Waha A, Pietsch (2013) H3F3A K27M mutation in pediatric CNS tumors: a marker for diffuse high-grade astrocytomas. *Am J Clin Pathol* **139**:345–349.
13. Grasso CS, Tang Y, Truffaux N, Berlow NE, Liu L, Debily MA *et al* (2015) Functionally defined therapeutic targets in diffuse intrinsic pontine glioma. *Nature Med* **21**:555–559.
14. Hashizume R, Andor N, Ihara Y, Lerner R, Gan H, Chen X *et al* (2014) Pharmacologic inhibition of histone demethylation as a therapy for pediatric brainstem glioma. *Nature Med* **20**:1394–1396.
15. Herz HM, Morgan M, Gao X, Jackson J, Rickels R, Swanson SK *et al* (2014) Histone H3 lysine-to-methionine mutants as a paradigm to study chromatin signaling. *Science* **345**:1065–1070.
16. Hochart A, Escande F, Rocourt N, Grill J, Koubi-Pick V, Beaujot J *et al* (2015) Long survival in a child with a mutated K27M-H3.3 pilocytic astrocytoma. *Ann Clin Transl Neurol* **2**:439–443.
17. Horbinski C, Miller CR, Perry A (2011) Gone FISHing: clinical lessons learned in brain tumor molecular diagnostics over the last decade. *Brain Pathol* **21**:57–73.
18. Huse JT, Nafa K, Shukla N, Kastenhuber ER, Lavi E, Hedvat CV, *et al* (2011) High frequency of IDH-1 mutation links glioneuronal tumors with neuropil-like islands to diffuse astrocytomas. *Acta Neuropathol* **122**:367–369.
19. Khuong-Quang DA, Buczkowicz P, Rakopoulos P, Liu XY, Fontebasso AM, Bouffet E *et al* (2012) K27M mutation in histone H3.3 defines clinically and biologically distinct subgroups of pediatric diffuse intrinsic pontine gliomas. *Acta Neuropathol* **124**: 439–447.
20. Korshunov A, Ryzhova M, Hovestadt V, Bender S, Sturm D, Capper D *et al* (2015) Integrated analysis of pediatric glioblastoma reveals a subset of biologically favorable tumors with associated molecular prognostic markers. *Acta Neuropathol* **129**:669–678.
21. Lewis PW, Muller MM, Koletsky MS, Cordero F, Lin S, Banaszynski LA *et al* (2013) Inhibition of PRC2 activity by a gain-of-function H3 mutation found in pediatric glioblastoma. *Science* **340**:857–861.
22. Mabray MC, Glastonbury CM, Mamlouk MD, Punch GE, Solomon DA, Cha S (2015) Direct cranial nerve involvement by gliomas: case series and review of the literature. *Am J Neuroradiol* **36**: 1349–1354.
23. Nguyen AT, Colin C, Nanni-Metellus I, Padovani L, Maurage CA, Varlet P *et al* (2015) Evidence for BRAF V600E and H3F3A K27M double mutations in paediatric glial and glioneuronal tumours. *Neuropathol Appl Neurobiol* **41**:403–408.

24. Reyes-Botero G, Giry M, Mokhtari K, Labussiere M, Idbaih A, Delattre JY *et al* (2014) Molecular analysis of diffuse intrinsic brainstem gliomas in adults. *J Neurooncol* **116**:405–411.
25. Schartzentruber J, Korshunov A, Liu XY, Jones DT, Pfaff E, Jacob K *et al* (2012) Driver mutations in histone H3.3 and chromatin remodelling genes in paediatric glioblastoma. *Nature* **482**:226–231.
26. Sturm D, Witt H, Hovestadt V, Khuong-Quang DA, Jones DT, Konermann C *et al* (2012) Hotspot mutations in H3F3A and IDH1 define distinct epigenetic and biological subgroups of glioblastoma. *Cancer Cell* **22**:425–437.
27. Taylor KR, Mackay A, Truffaux N, Butterfield YS, Morozova O, Phillippe C *et al* (2014) Recurrent activating ACVR1 mutations in diffuse intrinsic pontine gliomas. *Nature Genet* **46**:457–461.
28. Venneti S, Santi M, Felicella MM, Yarilin D, Phillips JJ, Sullivan LM *et al* (2014) A sensitive and specific histopathologic prognostic marker for H3F3A K27M mutant pediatric glioblastomas. *Acta Neuropathol* **128**:743–753.
29. Wu G, Broniscer A, McEachron TA, Lu C, Paugh BS, Becksfort J *et al* (2012) Somatic histone H3 alterations in pediatric diffuse intrinsic pontine gliomas and non-brainstem glioblastomas. *Nature Genet* **44**: 251–253.
30. Wu G, Diaz AK, Paugh BS, Rankin SL, Ju B, Li Y *et al* (2014) The genomic landscape of diffuse intrinsic pontine glioma and pediatric non-brainstem high-grade glioma. *Nature Genet* **46**:444–450.
31. Zhang L, Chen LH, Wan H, Yang R, Wang Z, Feng J *et al* (2014) Exome sequencing identifies somatic gain-of-function PPM1D mutations in brainstem gliomas. *Nature Genet* **46**:726–730.